Research Article | Vol. 29, No. 2 / 18 January 2021 / Optics Express 740
Optics EXPRESS

Experimental demonstration of a time-domain digital-coding metasurface for a Doppler cloak

BAIYANG LIU,[1,2] YEJUN HE,[1] SAI-WAI WONG,[1] AND YIN LI[1,3]

[1]College of Electronics and Information Engineering, Shenzhen University, Shenzhen, 518061, China
[2]State Key Laboratory of Millimeter Waves, Southeast University, Nanjing, 211189, China
[3]liyinuestc@gmail.com

Abstract: By generating an artificial Doppler shift, a Doppler cloak can compensate for the Doppler shift from a moving object. An object covered by a Doppler cloak will be detected as a static object, even if it is actually moving. Herein, we experimentally demonstrate the Doppler cloak in a radar system using a time-domain digital-coding metasurface. We theoretically illustrate an active metasurface with a modulated reflection phase that can imitate the motion of moving, thereby generating an artificial Doppler shift for a Doppler cloak. Moreover, a reflective metasurface composed of voltage-controlled varactor diodes with a 3-bit reflection phase was designed and fabricated. Finally, we experimentally demonstrate that an artificial Doppler shift for a Doppler cloak is obtained from the proposed metasurface using a discrete time-varying bias voltage. Simulation and measurement results show that the proposed time-domain digital-coding metasurface can cancel the Doppler shift and serve as a Doppler cloak. The proposed metasurface may have potential applications in a Doppler radar illusion, Doppler cancellation in vehicle-to-vehicle communications, and wireless communications.

1. Introduction

An object covered by an invisibility cloak is invisible from an external observer [1,2]. By using transformation optics [3,4], we can design the invisibility cloak explicitly. However, the invisibility cloaks based on the limited bandwidth metasurfaces are restricted to fundamental limitations. The invisible ability of a cloak can be defeated while it is in relativistic motion because of the Doppler effect. The Doppler effect may shift the incident signal outside its operating frequency. Hence, an invisibility cloak becomes visible by Doppler radar [5,6]. The Doppler effect is a well-known phenomenon that can be observed by acoustic or EM waves, which arise from a relativistic motion between a wave source and an external detector. To utilize the cloaking technique when in relativistic motion, the ability to cloak a moving object from a static observer has recently been studied, which is termed a Doppler cloak. A moving object covered by a space-time-modulated metamaterial has the ability to generate an opposite frequency shift to that from linear movement [7,8]. The Doppler radar will detect the object covered by a space-time-modulated metamaterial as stationary even though it is moving. In 2017, a metasurface with a time-varying transmission coefficient was theoretically designed as an artificial frequency translator, which is a potential candidate for a Doppler cloak [9].

Electromagnetic (EM) waves can be manipulated by metamaterials, which have been widely used to arbitrarily control the amplitude, phase shift, and polarization state of EM waves. Metasurfaces are two-dimensional metamaterials that have been widely investigated owing to their simple structure and low cost. Metasurfaces have been studied for many interesting applications, such as a negative refraction [10,11], invisibility cloak [12,13], flat lenses [14–16], and high-directivity antennas [17–19]. In addition, metasurfaces have been explored their space-time modulation ability by adding active components, such as varactor diodes, PIN diodes, and transistors. Metasurfaces with active unit cells have unique EM performances and properties that cannot be achieved by their passive counterparts. Active metasurfaces using reconfigurable

#414408 https://doi.org/10.1364/OE.414408
Journal © 2021 Received 6 Nov 2020; revised 21 Dec 2020; accepted 22 Dec 2020; published 4 Jan 2021

Optics EXPRESS

techniques have been proposed to obtain tunable functionalities such as operating frequency tunability [20–22], steerable polarization states [23–25], and dynamic scattering control [26–28], and have also been used to reduce the radar cross section (RCS) of antennas and reflectors [29,30]. Until recently, space-time engineered structures [31–34] were designed to generate harmonic frequencies [35–37], and time-varying metasurfaces have been verified to translate the illuminating waves [9,38]. Time-domain digital-coding metasurfaces have demonstrated the ability of nonlinear harmonic manipulation [39]. Moreover, the time-varying metasurfaces have been explored owing to their ability to achieve non-reciprocity in both microwaves and optics [40,41]. Time-varying metamaterials and metasurfaces have been used also to achieve nonreciprocal radiation from devices and compensation of Doppler effect also in antennas [42–46]. However, time-domain digital-coding metasurfaces have yet to be experimentally demonstrated for Doppler cloaks in a radar system.

In this paper, we experimentally demonstrate the Doppler cloak in a radar system using a time-domain digital-coding metasurface. We propose that a modulated reflection phase from an active metasurface has the same effect as linear movement generating a linear Doppler shift. An object covered by a time-modulated reflective metasurface can generate an artificial frequency shift to cancel the one from a linear movement, such that an observer, for example, a Doppler radar, detects the composite system as a static object even when it is moving. Moreover, a varactor-based metasurface with $21 \times 21 = 441$ active unit cells that can produce a 3-bit reflection phase response was designed and fabricated, and the prototype was tested. The reflection phase can be modulated periodically with an interval of 45° by tuning the capacitance of the varactor diodes. Because the reflection phase of the metasurface is periodically switched between eight different states, the propose that the metasurface can imitate a discrete linear movement and generate a dominant frequency shift for a Doppler cloak. The frequency shifts from the proposed metasurface with a 3-bit reflection phase were calculated and measured. An external observer, for example, Doppler radar, will detect the time-domain digital-coding metasurface with a certain velocity as stationary because the artificial frequency shift can compensate the one from linear movement. The active metasurface presented in this study may have potential applications in a Doppler radar illusion, Doppler cancellation in vehicle-to-vehicle communications, and wireless communications.

2. Theory

Consider that a Doppler radar generates an EM signal working at f_0 to a target and detects the scattered signal. For a normal incident, if the reflecting object is a metal reflector with a linear moving velocity v approaching the radar, the travel distance between the Doppler radar and metal reflector is $d(t) = d_0 - 2vt$, where t is the time variable, and d_0 is the travel distance at $t = 0$. Here, a positive and negative velocity means approaching and receding, respectively. The time-varying phase of the reflected signal owing to the linear movement velocity v is related to the travel distance $\phi_v(t) = -2\pi d(t)/\lambda_0$, where $\lambda_0 = c/f_0$ is the wavelength of the incident signal, and the speed of light is c. Therefore, the time-varying phase of the scattered signal is as follows:

$$\phi_v(t) = -\frac{2\pi d_0}{\lambda_0} + \frac{4\pi v t}{\lambda_0}. \tag{1}$$

The spectrum of the scattered signal with time-varying phase $E(t) = E_0 exp\{j\phi_v(t)\}$ can be calculated using the Fourier transform $\mathcal{F}\{E(t)\}$, which has a well-known Doppler shift $\Delta f_{\phi_v} = 2vf_0/c$, as shown in Fig. 1(A).

Herein, we propose an active metasurface with a modulated reflection phase $\phi_m(t)$ to compensate for the time-varying phase $\phi_v(t)$ from a linear movement, that is, $\phi_m(t) + \phi_v(t) = 0$, and then generate an opposite artificial Doppler shift Δf_{ϕ_m} to the one from the linear movement Δf_{ϕ_v}, the overall frequency shift is $\Delta f_{\phi_m} + \Delta f_{\phi_v} = 0$, as shown in Fig. 1(b). Such an active metasurface

Optics EXPRESS

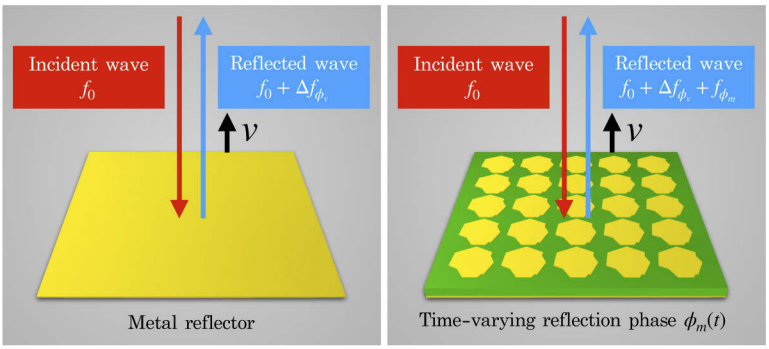

(a) (b)

Fig. 1. (a) A metal reflector with a linear moving velocity v has a frequency shift Δf_{ϕ_v}, which is the well-known Doppler effect. (b) An active metasurface with a linear moving velocity v and a modulated reflection phase $\phi_m(t)$ generates an artificial Doppler shift, which has an overall frequency shift $\Delta f_{\phi_v} + \Delta f_{\phi_m}$. In particular, $\Delta f_{\phi_v} + \Delta f_{\phi_m} = 0$, an active metasurface, can be used as a Doppler cloak.

with a zero-frequency shift can be used as a Doppler cloak. An object covered by the proposed metasurface is detected as a static object despite actually moving.

3. Coding metasurface using varactor diodes

To verify the proposed theory, a metasurface operating at 5.8 GHz with $21 \times 21 = 441$ active unit cells incorporating voltage-controlled varactor diodes (SMV2019-079LF) is designed and fabricated, as shown in Fig. 2. The top and bottom metal layers are printed on a substrate layer (Rogers RT5880), with a dielectric constant and loss tangent of 2.2 and 0.0009, respectively. The design details of the unit cell are shown in Figs. 3(A) and 3(b) for top and side views, respectively. The overall size of the proposed metasurface is 240×240 mm. All varactor diodes are connected to the + and - of the bias line with a simple biasing network, and a small gap of $0.2mm$ on the bottom layer is used to separate the + and -, although the device still behaves as a ground plane. In our simulation, the varactor diode is considered an RLC cascade circuit model at the operating frequency. The equivalent circuit model of the unit cell can be found in [47]. A time-varying external voltage $U(t)$ is used to generate a time-domain digital-coding modulated reflection phase. By tuning the external voltage, the proposed active metasurface obtains eight different states, denoted as S1-S8, where each state is encoded by a binary code. The metasurface can produce a 3-bit reflection phase response, that is, the full 360° is equally divided into eight states, and every adjacent state has a phase difference of 45°. Here, the reflection phase response of the proposed metasurface is designed for a normal incident y-polarization at 5.8 GHz, as shown in Fig. 3.

The reflection phase of the metasurface is obtained by measuring the transmission between two horn antennas in an anechoic chamber. The measurement setup is shown in Fig. 4(A). Two horn antennas as a transmitter and receiver are connected to a Keysight E5071C network analyzer, both of which are 1 m from the metasurface, and a direct-current (DC) power supply is used to bias the varactor diodes. The reflection measurement was calibrated using a copper plate. The measured reflection responses with different bias voltages are shown in Fig. 4(b), where a required 315° phase difference is obtained. The capacitance C_p of the varactor diode is changed by the bias voltage within the range from 0.37 to 0.55 pF. For more information, please check the data sheet of SMV2019-079LF. Table 1 details the measured reflection response at 5.8 GHz; thus, we can obtain the phase intervals of adjacent states as 43°, 46°, 45°, 45°, 47°, 43°, 45°, and

Optics EXPRESS

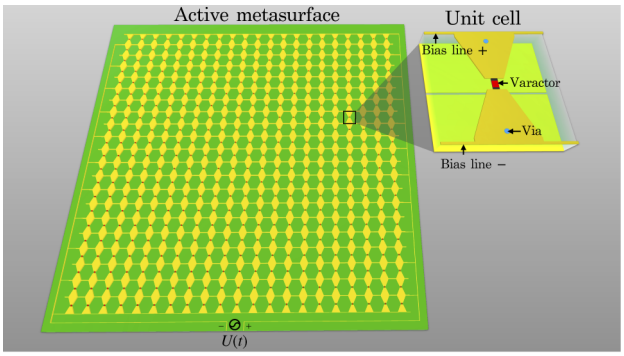

(a)

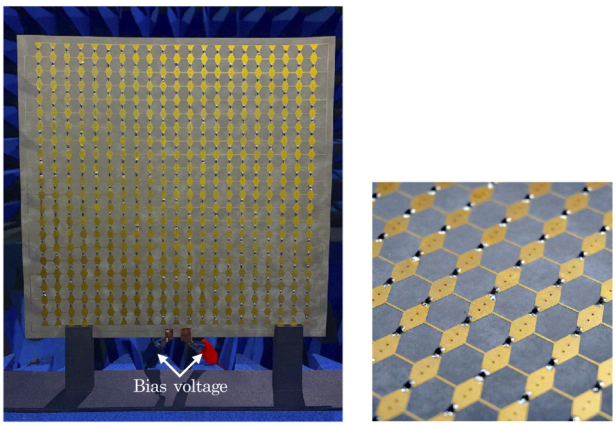

(b)

Fig. 2. (a) Design of the proposed active metasurface with $21 \times 21 = 441$ unit cells for a Doppler cloak. The bias voltage is provided by the + and - of the bias line on each unit cell, and the metasurface is connected to a time-domain digital-coding bias voltage $U(t)$ through a simple biasing network. (b) Fabricated prototype. All varactor diodes are soldered using surface mounting technology.

46°, respectively, which are in good agreement with the expected interval of 45°. The measured reflection amplitude is not at the same level, but such a difference in the reflection amplitude does not affect the ability of the proposed metasurface to translate the reflected signal. Therefore, the 3-bit reflection phase can be time-domain digitally coded by the external voltage $U(t)$.

Optics EXPRESS

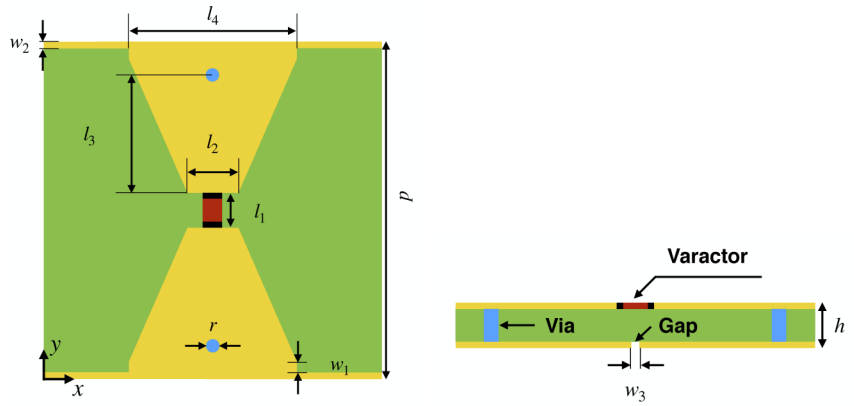

(a) (b)

Fig. 3. Design parameters of the proposed metasurface. (a) Top view of the unit cell. (b) Side view of the unit cell h = 0.5 mm, p = 10 mm, w_1 = 0.3 mm, w_2 = 0.2 mm, w_3 = 0.2 mm, l_1 = 1 mm, l_2 = 1.5 mm, l_3 = 3.5 mm, l_4 = 5 mm, and r = 0.4 mm. The capacitance of the varactor diode on the unit cell ranges from 0.30 to 2.22 pF. The proposed metasurface is designed for y-polarization at 5.8 GHz.

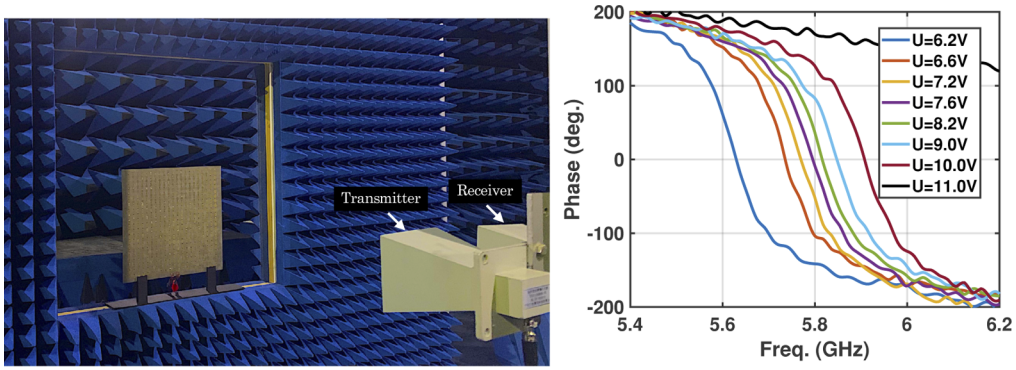

(a) (b)

Fig. 4. (a) Reflection response measurement setup. (b) Measured reflection phases with different bias voltages.

Table 1. Measured reflection responses with different bias voltages at 5.8 GHz

State	Binary code	Bias voltage	Refl. phase	Refl. amplitude
S1	000	6.2 V	27°	0.92
S2	001	6.6 V	70°	0.92
S3	010	7.2 V	116°	0.83
S4	011	7.6 V	161°	0.82
S5	100	8.2 V	206°	0.86
S6	101	9.0 V	253°	0.90
S7	110	10.0 V	296°	0.92
S8	111	11.0 V	341°	0.94

Optics EXPRESS

4. 3-bit time-domain digital-coding metasurface for doppler cloak

Consider that the 3-bit reflection phase of the proposed metasurface is decreased sequentially and periodically such that each state is switched on for a time period given by $\tau_s = T_s/8$, where T_s is the overall sequence switching period. Here, we denote the 3-bit reflection response as $\phi_d(t)$, which is the discrete form of an ideal reflection phase $\phi_m(t) = -\phi_v(t)$, to cancel the Doppler shift from linear motion, as shown in Fig. 5(A). Using the time-domain digital-coding reflection phase, we can imitate the motion of a recession from the observer to compensate the Doppler shift from the approaching linear movement. A Fourier analysis is used to calculate the spectrum $E_r(\omega)$ of the reflected signal from the proposed metasurface with the $\phi_d(t)$ reflection phase:

$$E_r(\omega) = \int_{-\infty}^{+\infty} E_0 exp\{j\phi_d(t)\} exp(-j\omega t)dt. \tag{2}$$

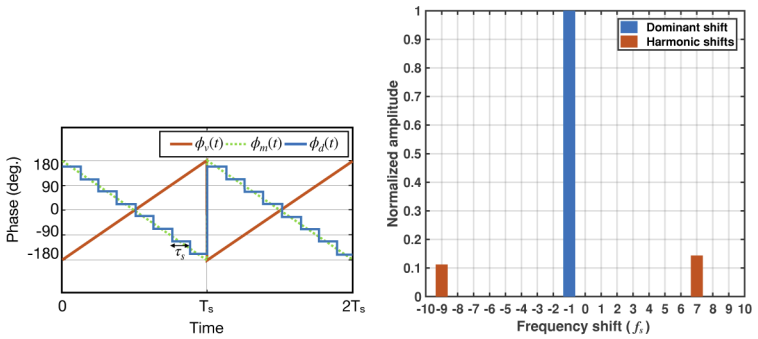

Fig. 5. (a) The red line is the time-varying phase $\phi_v(t)$ from linear movement that generates a Doppler shift. The green-dashed line is the ideal modulated reflection phase $\phi_m(t) = -\phi_v(t)$ to compensate for the Doppler shift from linear movement. The blue line is the proposed 3-bit reflection phase $\phi_d(t)$ of our coding metasurface for the Doppler cloak. (b) Calculated frequency shifts of the reflected signal from the proposed metasurface with the time-domain digital-coding reflection phase $\phi_d(t)$.

Therefore, the reflected wave can be expressed as a Fourier series, where a_k is the harmonic coefficient

$$E_r(t) = \sum_{k=-\infty}^{+\infty} a_k exp(jk\frac{2\pi}{T_s}t) exp(j2\pi f_0 t). \tag{3}$$

The calculated spectrum is shown in Fig. 5(b), where a dominant frequency shift at $\Delta f = -f_s = -1/T_s$ is obtained. The low power harmonic frequency shifts are also observed in the spectrum whose normalized amplitudes are lower than 0.15.

Herein, we experimentally demonstrate that the proposed metasurface can be used as a frequency translator. To realize the discrete reflection phase $\phi_d(t)$ shown in Fig. 5(A) by the active metasurface, a discrete coding voltage is required. We used the experimental setup shown in Fig. 6 in an anechoic chamber to measure the artificial Doppler shift, the proposed metasurface is biased by an arbitrary waveform generator with a discrete coding voltage $U(t)$. Different voltages of 6.2, 6.6, 7.2, 7.6, 8.2, 9.0, 10.0, and 11.0 V are coded with a binary code based on Table 1 and repeated periodically, as shown in Fig. 7(A), which is measured using an oscilloscope, of which the additive noise level is less than 0.06 V. Here, we demonstrate the coding metasurface as a reflective frequency translator for two different frequency shifts. The frequency of the discrete time-varying voltage is $f_1 = 1$ MHz and $f_2 = 2$ MHz, respectively. A signal generator

Optics EXPRESS

(Aiglent N5172B) is connected to the transmitting antenna with a −10 dBm signal at 5.8 GHz, and the receiving antenna is connected to a signal analyzer (Agilent 9020B) to measure the frequency shifts. As shown in Fig. 7(b), two different dominant frequency shifts $\Delta f_1 = -1$ MHz and $\Delta f_2 = -2$ MHz are measured, respectively, which have a good agreement with the theoretical results. The calculated low-power harmonic frequency shifts in Fig. 5(b) are not clearly detected owing to the transmission loss and environmental noise.

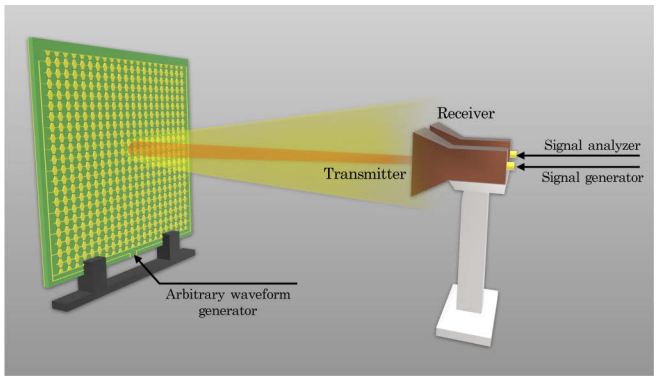

Fig. 6. Experiment setup used to measure the frequency shifts from the proposed coding metasurface.

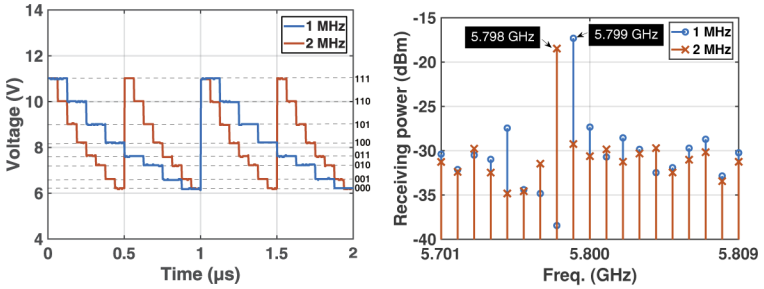

(a) (b)

Fig. 7. (a) Measured discrete time-varying bias voltage for the proposed coding metasurface. (b) Measured spectrum of the signal reflected by the proposed metasurface.

In addition, we experimentally demonstrate that the proposed time-domain digital-coding metasurface has the ability to deceive Doppler radar. In our experiment, the time-domain digital-coding metasurface was controlled by an arbitrary waveform generator with a discrete time-varying voltage as shown in Fig. 7(A). A Doppler radar with a linear movement velocity was used as an external observer, and the spectrograms of the signal reflected by the proposed metasurface were measured. BumbleBee radar is a low-power pulsed Doppler radar operating at 5.8 GHz, and its detection range reaches up to 8 m [48]. The experimental setup to demonstrate the Doppler cloak using the proposed metasurface is shown in Fig. 8(A). The Doppler radar was moved by a linear slide rail with a speed controllable stepper motor, and the moving velocity can be controlled by a remote control. In our experiment, we measured the spectrograms in two different cases. In Case 1, a copper plate is used as a reflector, the Doppler radar approaches the reflector linearly with a velocity of +0.62 m/s and duration of 1 s, and the linear Doppler shift owing to this linear movement can be calculated using $\Delta f_{linear} = 2vf_0/c = 23.97$ Hz, which is measured as shown in Fig. 8(b). The initial distance between the radar and reflector is 1.5 m, and

Optics EXPRESS

the ending distance is 1.5-0.62=0.88 m. Note that not all the scattered signals are with frequency translation, the scattered signals are inevitably reflected by other objects. The zero-frequency shift shown in Fig. 8(b) is caused by the signals reflected by the objects relative static to the Doppler radar. In Case 2, the copper plate is replaced by the proposed time-domain digital-coding metasurface with a modulated bias voltage, and the Doppler radar still moves forward linearly toward the reflector with a velocity of +0.62 m/s and duration of 1 s. For a Doppler radar system operating at f_0, to compensate the linear Doppler shift Δf_{linear} by a time-domain digital-coding metasurface, which generates a dominant frequency shift Δf_{mod}, that is, $\Delta f_{mod} = -\Delta f_{linear}$, the

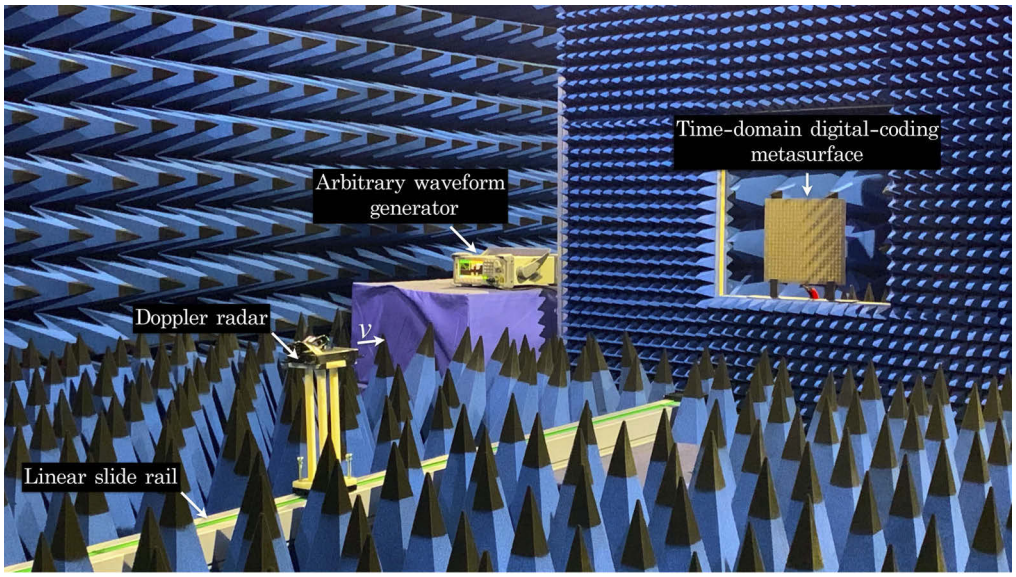

(a)

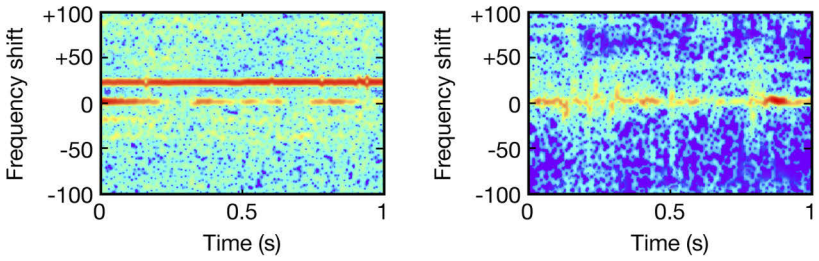

(b) (c)

Fig. 8. (a) Experiment using Doppler cloak by the time-domain digital-coding metasurface. A Doppler radar approaches the metasurface with a linear velocity, and the metasurface was modulated by an arbitrary waveform generator with a discrete time-varying voltage to generate an opposite artificial Doppler shift. Hence, we can obtain a zero-frequency shift to demonstrate the Doppler cloak concept. (b) Case 1: Measured spectrogram of a copper plate as a reflector. The Doppler radar with a linear movement velocity of +0.62 m/s, an expected approximate Doppler shift of 23.97 Hz is measured. (c) Case 2: Measured spectrogram of proposed metasurface as a reflector. The modulated frequency of the bias voltage was set to 23.97 Hz, whereas for Doppler radar with a linear movement velocity of +0.62 m/s, the artificial Doppler shift cancels the Doppler shift from the linear movement, and therefore a zero-frequency shift is therefore obtained.

Optics EXPRESS

modulated frequency of the discrete time-varying bias voltage should be $f_s = \Delta f_{linear} = 23.97$ Hz. The periodical decreased reflection phase can mimic the motion of a recession and therefore compensate for the Doppler shift from the motion of approach. The measured zero-frequency shift from the spectrogram, as shown in Fig. 8(c), proves that the proposed metasurface can be used as a Doppler cloak. The imperfect spectrogram in Fig. 8(c) is due to the metasurface being designed for a normal small-angle incidence, and therefore not all reflected waves are modulated by the metasurface.

5. Conclusion

In this study, we experimentally presented an active reflective metasurface with a proper time-varying reflection phase that can be designed as a Doppler cloak. We have theoretically extracted the necessary reflection phase conditions to compensate for the Doppler shift from linear moving. A metasurface composed of $21 \times 21 = 441$ voltage-controlled varactor diodes with a 3-bit reflection phase is designed and fabricated. Using a 3-bit coding strategy, the harmonic frequency shifts are suppressed. When discrete reflection phase states of the metasurface are coded by binary sequences, one can control the artificial frequency shift of the reflected signal by using elaborate coding strategies. Moreover, by changing the modulation frequency of the reflection phase, the proposed active metasurface can induce an arbitrary frequency shift, and the output velocity of a Doppler radar can be controlled, that is, a Doppler radar illusion occurs. In summary, the proposed time-domain digital-coding metasurface is a potential candidate for use in a Doppler cloak, Doppler radar illusion, Doppler cancellation in vehicle-to-vehicle communications, and wireless communications.

Funding. National Natural Science Foundation of China (62071306); China Postdoctoral Science Foundation (2020M682876); Guangdong Basic and Applied Basic Research Foundation (2019A1515111127); the State Key Laboratory of the Millimeter Waves Foundation (K202113); the Shenzhen Science and Technology Program (JCYJ20180305124543176, JCYJ20190808145411289); Natural Science Foundation of Guangdong Province (2018A030313481); Shenzhen University Research Startup Project of the New Staff (860-000002110311).

Disclosures. The authors declare no conflicts of interest.

References

1. R. Liu, C. Ji, J. Mock, J. Chin, T. Cui, and D. Smith, "Broadband ground-plane cloak," Science **323**(5912), 366–369 (2009).
2. W. Cai, U. K. Chettiar, A. V. Kildishev, and V. M. Shalaev, "Optical cloaking with metamaterials," Nat. Photonics **1**(4), 224–227 (2007).
3. J. B. Pendry, D. Schurig, and D. R. Smith, "Controlling electromagnetic fields," Science **312**(5781), 1780–1782 (2006).
4. H. Chen, C. T. Chan, and P. Sheng, "Transformation optics and metamaterials," Nat. Mater. **9**(5), 387–396 (2010).
5. J. C. Halimeh, R. T. Thompson, and M. Wegener, "Invisibility cloaks in relativistic motion," Phys. Rev. A **93**(1), 013850 (2016).
6. B. Liu, H. Chu, H. Giddens, R. Li, and Y. Hao, "Experimental observation of linear and rotational doppler shifts from several designer surfaces," Sci. Rep. **9**(1), 8971 (2019).
7. D. Ramaccia, D. L. Sounas, A. Alù, A. Toscano, and F. Bilotti, "Doppler cloak restores invisibility to objects in relativistic motion," Phys. Rev. B **95**(7), 075113 (2017).
8. B. Liu, H. Giddens, Y. Li, Y. He, S.-W. Wong, and Y. Hao, "Design and experimental demonstration of doppler cloak from spatiotemporally modulated metamaterials based on rotational doppler effect," Opt. Express **28**(3), 3745–3755 (2020).
9. D. Ramaccia, D. L. Sounas, A. Alù, A. Toscano, and F. Bilotti, "Phase-induced frequency conversion and doppler effect with time-modulated metasurfaces," IEEE Trans. Antennas Propag. **68**(3), 1607–1617 (2020).
10. R. A. Shelby, D. Smith, S. Nemat-Nasser, and S. Schultz, "Microwave transmission through a two-dimensional, isotropic, left-handed metamaterial," Appl. Phys. Lett. **78**(4), 489–491 (2001).
11. R. A. Shelby, D. R. Smith, and S. Schultz, "Experimental verification of a negative index of refraction," Science **292**(5514), 77–79 (2001).
12. H. Chen, B.-I. Wu, B. Zhang, and J. A. Kong, "Electromagnetic wave interactions with a metamaterial cloak," Phys. Rev. Lett. **99**(6), 063903 (2007).
13. D. Schurig, J. J. Mock, B. Justice, S. A. Cummer, J. B. Pendry, A. F. Starr, and D. R. Smith, "Metamaterial electromagnetic cloak at microwave frequencies," Science **314**(5801), 977–980 (2006).

Optics EXPRESS

14. C. Pfeiffer and A. Grbic, "A printed, broadband luneburg lens antenna," IEEE Trans. Antennas Propag. **58**(9), 3055–3059 (2010).
15. Q. Cheng, H. F. Ma, and T. J. Cui, "Broadband planar luneburg lens based on complementary metamaterials," Appl. Phys. Lett. **95**(18), 181901 (2009).
16. F. Aieta, P. Genevet, M. A. Kats, N. Yu, R. Blanchard, Z. Gaburro, and F. Capasso, "Aberration-free ultrathin flat lenses and axicons at telecom wavelengths based on plasmonic metasurfaces," Nano Lett. **12**(9), 4932–4936 (2012).
17. G. Minatti, M. Faenzi, E. Martini, F. Caminita, P. De Vita, D. González-Ovejero, M. Sabbadini, and S. Maci, "Modulated metasurface antennas for space: Synthesis, analysis and realizations," IEEE Trans. Antennas Propag. **63**(4), 1288–1300 (2015).
18. A. Ghasemi, S. N. Burokur, A. Dhouibi, and A. de Lustrac, "High beam steering in fabry–pérot leaky-wave antennas," Antennas Wirel. Propag. Lett. **12**, 261–264 (2013).
19. A. Epstein, J. P. Wong, and G. V. Eleftheriades, "Cavity-excited huygens' metasurface antennas for near-unity aperture illumination efficiency from arbitrarily large apertures," Nat. Commun. **7**(1), 10360 (2016).
20. B. Sanz-Izquierdo and E. A. Parker, "Dual polarized reconfigurable frequency selective surfaces," IEEE Trans. Antennas Propag. **62**(2), 764–771 (2014).
21. P. S. Taylor, E. A. Parker, and J. C. Batchelor, "An active annular ring frequency selective surface," IEEE Trans. Antennas Propag. **59**(9), 3265–3271 (2011).
22. W. Xu, Y. He, P. Kong, J. Li, H. Xu, L. Miao, S. Bie, and J. Jiang, "An ultra-thin broadband active frequency selective surface absorber for ultrahigh-frequency applications," J. Appl. Phys. **118**(18), 184903 (2015).
23. G. Du, C. Yu, and C. Liu, "Frequency selective surface with switchable polarization," Microw. Opt. Technol. Lett. **56**(2), 515–518 (2014).
24. W. Li, S. Xia, B. He, J. Chen, H. Shi, A. Zhang, Z. Li, and Z. Xu, "A reconfigurable polarization converter using active metasurface and its application in horn antenna," IEEE Trans. Antennas Propag. **64**(12), 5281–5290 (2016).
25. B. Ratni, A. de Lustrac, G.-P. Piau, and S. N. Burokur, "Electronic control of linear-to-circular polarization conversion using a reconfigurable metasurface," Appl. Phys. Lett. **111**(21), 214101 (2017).
26. H. Yang, X. Cao, F. Yang, J. Gao, S. Xu, M. Li, X. Chen, Y. Zhao, Y. Zheng, and S. Li, "A programmable metasurface with dynamic polarization, scattering and focusing control," Sci. Rep. **6**(1), 35692 (2016).
27. B. O. Zhu, K. Chen, N. Jia, L. Sun, J. Zhao, T. Jiang, and Y. Feng, "Dynamic control of electromagnetic wave propagation with the equivalent principle inspired tunable metasurface," Sci. Rep. **4**(1), 4971 (2015).
28. X. Wan, M. Q. Qi, T. Y. Chen, and T. J. Cui, "Field-programmable beam reconfiguring based on digitally-controlled coding metasurface," Sci. Rep. **6**(1), 20663 (2016).
29. Y. Liu, K. Li, Y. Jia, Y. Hao, S. Gong, and Y. J. Guo, "Wideband rcs reduction of a slot array antenna using polarization conversion metasurfaces," IEEE Trans. Antennas Propag. **64**(1), 326–331 (2016).
30. Y. Jia, Y. Liu, Y. J. Guo, K. Li, and S.-X. Gong, "Broadband polarization rotation reflective surfaces and their applications to rcs reduction," IEEE Trans. Antennas Propag. **64**(1), 179–188 (2016).
31. J. Y. Dai, J. Zhao, Q. Cheng, and T. J. Cui, "Independent control of harmonic amplitudes and phases via a time-domain digital coding metasurface," Light: Sci. Appl. **7**(1), 90 (2018).
32. L. Zhang, X. Q. Chen, S. Liu, Q. Zhang, J. Zhao, J. Y. Dai, G. D. Bai, X. Wan, Q. Cheng, G. Castaldi, V. Galdi, and T. J. Cui, "Space-time-coding digital metasurfaces," Nat. Commun. **9**(1), 4334 (2018).
33. J. Y. Dai, W. Tang, L. X. Yang, X. Li, M. Z. Chen, J. C. Ke, Q. Cheng, S. Jin, and T. J. Cui, "Realization of multi-modulation schemes for wireless communication by time-domain digital coding metasurface," IEEE Trans. Antennas Propag. **68**(3), 1618–1627 (2020).
34. L. Zhang, Z. X. Wang, R. W. Shao, J. L. Shen, X. Q. Chen, X. Wan, Q. Cheng, and T. J. Cui, "Dynamically realizing arbitrary multi-bit programmable phases using a 2-bit time-domain coding metasurface," IEEE Trans. Antennas Propag. **68**(4), 2984–2992 (2020).
35. N. Chamanara, S. Taravati, Z.-L. Deck-Léger, and C. Caloz, "Optical isolation based on space-time engineered asymmetric photonic band gaps," Phys. Rev. B **96**(15), 155409 (2017).
36. S. Taravati and G. V. Eleftheriades, "Generalized space-time-periodic diffraction gratings: Theory and applications," Phys. Rev. Appl. **12**(2), 024026 (2019).
37. S. Taravati and A. A. Kishk, "Advanced wave engineering via obliquely illuminated space-time-modulated slab," IEEE Trans. Antennas Propag. **67**(1), 270–281 (2019).
38. Z. Wu and A. Grbic, "Serrodyne frequency translation using time-modulated metasurfaces," IEEE Trans. Antennas Propag. **68**(3), 1599–1606 (2020).
39. J. Zhao, X. Yang, J. Y. Dai, Q. Cheng, X. Li, N. H. Qi, J. C. Ke, G. D. Bai, S. Liu, S. Jin, A. Alú, and T. J. Cui, "Programmable time-domain digital-coding metasurface for non-linear harmonic manipulation and new wireless communication systems," Natl. Sci. Rev. **6**(2), 231–238 (2019).
40. A. Shaltout, A. Kildishev, and V. Shalaev, "Time-varying metasurfaces and lorentz non-reciprocity," Opt. Mater. Express **5**(11), 2459–2467 (2015).
41. Y. Hadad, D. Sounas, and A. Alu, "Space-time gradient metasurfaces," Phys. Rev. B **92**(10), 100304 (2015).
42. D. Ramaccia, D. L. Sounas, A. Alù, F. Bilotti, and A. Toscano, "Nonreciprocal horn antennas using angular momentum-biased metamaterial inclusions," IEEE Trans. Antennas Propag. **63**(12), 5593–5600 (2015).
43. D. Ramaccia, D. L. Sounas, A. Alù, F. Bilotti, and A. Toscano, "Nonreciprocity in antenna radiation induced by space-time varying metamaterial cloaks," Antennas Wirel. Propag. Lett. **17**(11), 1968–1972 (2018).

Optics EXPRESS

44. S. Taravati and C. Caloz, "Space-time modulated nonreciprocal mixing, amplifying and scanning leaky-wave antenna system," in *2015 IEEE International Symposium on Antennas and Propagation & USNC/URSI National Radio Science Meeting*, (IEEE, 2015), pp. 639–640.
45. Y. Hadad, J. C. Soric, and A. Alu, "Breaking temporal symmetries for emission and absorption," Proc. Natl. Acad. Sci. **113**(13), 3471–3475 (2016).
46. D. Ramaccia, D. L. Sounas, A. Marini, A. Toscano, and F. Bilotti, "Electromagnetic isolation induced by time-varying metasurfaces: Non-reciprocal bragg grating," Antennas Wirel. Propag. Lett. **19**(11), 1886–1890 (2020).
47. X. Gao, W. L. Yang, H. F. Ma, Q. Cheng, X. H. Yu, and T. J. Cui, "A reconfigurable broadband polarization converter based on an active metasurface," IEEE Trans. Antennas Propag. **66**(11), 6086–6095 (2018).
48. Samraksh Co. Website for the BumbleBee Radar, Online Available: https://samraksh.com/products/sensors/32-product-pages/products-sensors/71-bumblebee-radar. (2015).